JNBT
©2006INBDK

JNBT, Vol 3, No 1, pp. 30-35

Nano elastic memory using carbon nanocoils

Joo Han Chang[a] and Wanjun Park*

Materials and Devices Research Center, Samsung Advanced Institute of Technology 14-1 Giheung, Gyeonggi-Do 449-712 , Korea

ABSTRACT

We propose a novel non-volatile random access memory structure using the carbon nanocoil as the electromechanical switching device. Molecular simulations were performed to compute the range of dimensions for which the device is expected to exhibit non-volatility. Minimum operating voltages were also calculated through exhaustive electromagnetic simulations using the finite element method. It was found that the switching voltages can be as low as 1 V and 1.5 V for write and erase, respectively. The extent of electric crosstalk and the effect of nanocoil inductance were also investigated. The minimal power consumption level and the nanoscale dimensions of the carbon nanocoil make this structure a promising candidate for next generation-nanoelectronics.

Key words : carbon nanotube, non-volatile memory, carbon nanocoil

Introduction

Since its discovery in 1991 (1), carbon nanotubes have attracted much attention as a promising candidate for future nanoelectronics. Especially interesting among its many applications are electromechanical devices, including non-volatile random access memory (2), actuators (3), switches (4), gears (5), and nanotweezers (6), as studied by various investigators. One type of carbon nanotubes is the carbon nanocoil (CNC). Due to its startling helical structure at the nano-scale, the carbon nanocoil has many potential applications in a number of fields, including resonating elements, reinforcement in high-strain composites, nano solenoids and receivers. We propose a novel carbon nanocoil-based electromechanical and nonvolatile random access memory structure which is easily scaleable to the terabit/cm^2 level.

Carbon nanocoils are formed during the CVD synthesis process as shown in Fig 1 by a regular occurrence of particular defects in carbon nanotubes (7). Due to such complex a structure, the finding of carbon nanocoils had been considered to be extremely accidental. However, with increasing research in the domain, carbon nanocoils can now be consistently synthesized with a yield of over 90% (8, 9) and a diameter under 10 nm (10). Furthermore, there has been original yet underex-

Fig 1. SEM image of a vertically grown carbon nanocoil, whose diameter is under 100 nm. Such nanocoils can be exploited for ultra-high density nanoelectronics.

[a]Present address: Department of Electrical Engineering, Columbia University
* Corresponding author :
Wanjun Park
Tel : +82-31-280-9305
Fax : +82-31-280-9308
E-mail : wanjun@samsung.com

plored attempts at the patterned synthesis of the material, (11, 12) just like CNTs can be synthesized with nearly perfect order in AAO templates (13). Especially encouraging among recent endeavors was Bajpai *et al.*'s success in the large-scale synthesis of vertically self-aligned carbon nanocoils (14), which opened new horizons for carbon nanocoil synthesis and made carbon nanocoil applications ever closer to reality.

Structure and Device Operation

In light of the upward trend in the sophistication in CNC synthesis, our model for ultra-high density nonvolatile RAM employs a 2D array of vertically grown carbon nanocoils between a conventional cross-point array (15, 16), with some space intentionally allowed between the CNC in its natural state and the top electrode (Fig 2). An insulating layer such as SiO2 serves as the support for top electrodes and a template for CNC synthesis. Here we propose a memory core cell with the carbon nanocoils and its functional operations with write, erase, and read mode as shown in Fig 3 where each mode is controlled by the appropriate bias voltage. The governing forces of this memory cell system can be simplified as the summation of electromagnetic force, van der Waals force, and elastic force.

Despite their incredibly small size, carbon nanocoils were previously shown to exhibit the mechanical properties of a macroscale spring, with a constant spring constant K in the low strain region (17,18). Thus the elastic energy of a CNC can be effectively modeled using Hooke's law E = 0.5 kx^2. Furthermore, previous studies of CNC mechanics have shown that CNCs have a very low spring constant, with all K measurements falling under 1 N/m and indicated a slightly positive correlation between K and the coil radius, which agrees with the conventional spring theory, since the tube diameter is proportional to the coil radius: (17)

$$K = \frac{Gd^4}{64R^3N}$$

where d, R and N represent tube diameter, coil radius, and number of turns, respectively.

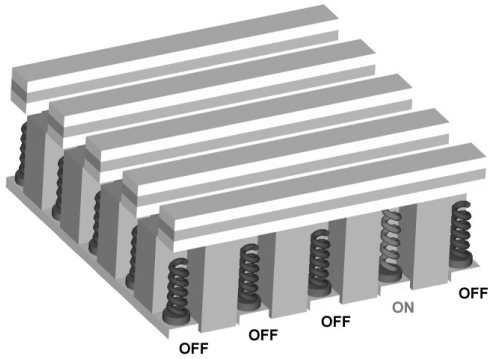

Fig 2. Cross-point array of carbon nanocoils for nonvolatile memory application. The nanocoil colored in red is stretched via Coulomb force and held by Van der Waals' force.

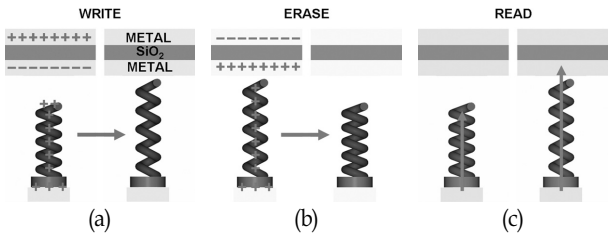

Fig 3. The proposed method for memory operation (a) Write Mode: Voltages of opposite polarity is applied to the lower and middle electrode. The resulting Coulomb force stretches the nanocoil. CNC stays bonded to the middle electrode, trapped in the potential well. (b) Erase Mode: Unipolar voltages are applied to the lower and middle electrode. The resulting Coulomb force relaxes the nanocoil to its original state. The induced charges in the top electrode help the accumulation of charges. (c) Read Mode: Data can be read by measuring the resistance of the system. As carbon nanocoils have conductivity values of ~180 S/cm, an excellent on/off ratio is expected.

The OFF state is represented by the separation between the nanocoil and electrode. The device can be switched to the ON state by applying voltages of opposite polarity to the upper and lower electrodes, and can be switched back to the OFF state by applying unipolar voltages. Fig 3 shows a proposed device with a capacitor based top-electrode to describe easily the electrostatics of the writing and erase mode. For the data writhing mode, a positive bias induces negative charges on the electrode that full the CNC charged positively by the positive bias. Once the CNC contacts with the top-electrode, van der Waals force holds the CNC to stay the ON state. For the data erase mode, while a negative bias induces positive charges on the electrode and on the CNC,

the CNC and top-electrode is separated and resulted to the OFF state when the electrostatic and elastic repulsion force is larger than van der Waals force. It should be noted that due to the high contact resistance between the nanocoil and the metal electrode (19), the nanocoil and the electrode are not at equipotential until the bias is applied to not one but both electrodes during erase mode. Bistability, or non-volatility, is achieved by the attractive Van der Waals energy when a nanocoil is stretched to the sub-nm separation region with the metal electrode. Its magnitude can be modeled through the Lennard-Jones 6-12 potential, which is given by the following expression: (20)

$$\Phi(r) = \varepsilon\left(\left(\frac{\sigma}{r}\right)^{12} - \left(\frac{\sigma}{r}\right)^{6}\right)$$

Molecular Simulation and Results

To calculate the contribution of Van der Waals' energy to the total potential energy of a single memory cell, a simplified molecular model of a carbon nanocoil 12 nm in length and 5 nm in diameter, in agreement with the diameter of the smallest reported carbon nanocoil (10), was created using alkene species. Based on this model, models of carbon nanocoils in a continuum of either compressed or stretched states, ranging from 80% to 120%, were generated. Cobalt was arbitrarily chosen as the electrode material for the simulation, whose crystal's molecular model was generated and appended to the CNC models as shown in Fig 4. To calculate the VdW energy, we chose TINKER Molecular Modeling Package, developed at University of Washington at St. Louis, which was previously used to investigate the VDW interaction between carbon nanotubes and contact surfaces (21). Finally, simulations were run on TINKER using MM2 parameters.

The result of this simulation on 200 different states of the system, taking the separation between the CNC and Co electrode as the variable, is shown in Fig 5. The plot clearly shows two local minima in the total potential energy curve, one due to the CNC's natural elastic state and the other due to the strong attractive force in the sub-nm separation region. The existence of two local minima translates into the

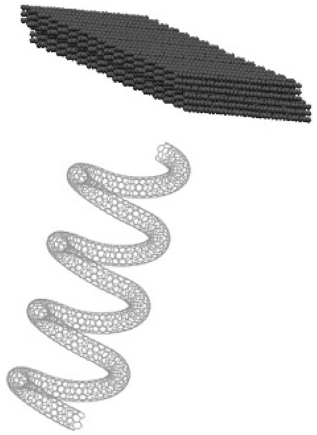

Fig 4. Molecular model of the carbon nanocoil - Co electrode system, rendered in TINKER Force Field Explorer. The top dielectric and uppermost electrode was not included as their effect on the VdW energy is negligible.

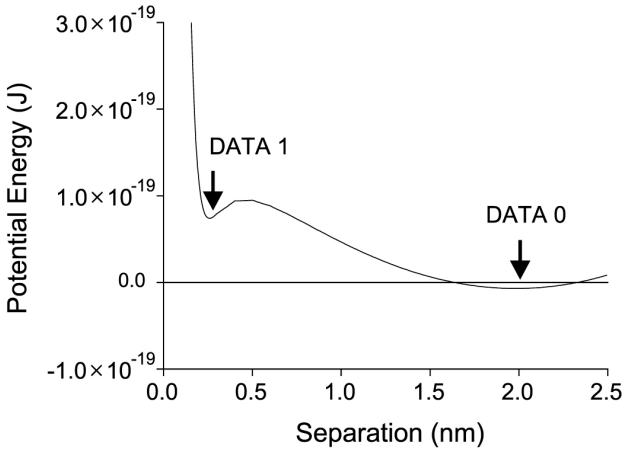

Fig 5. VdW energy simulation result summed with the elastic energy to obtain the total potential energy. It is seen that two local minima are present with a potential barrier on the order of 10^{-19} J.

bistability of the system, which can be readily exploited to fabricate a non-volatile random access memory.

However, it is impossible to engineer the dimensions of every cell precisely to the ones used in the above simulation. To extrapolate this result to all dimensions, we calculated the range of dimensions at which the CNC-electrode system exhibits bistability. Three variables, namely the coil diameter, initial separation, and coil spring constant, need to be satisfied to form a nonvolatile memory cell. The plot of the dimensions allowed in Fig 6 proves that this structure can tolerate a significant amount of deviation in cell dimensions,

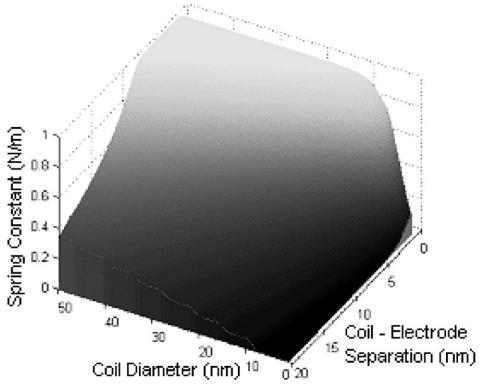

Fig 6. A 3-D plot of allowed spring constant, coil diameter and initial coil-electrode separation. Any dimensions that lies under the shown surface forms a valid memory cell.

which is favorable for device fabrication. It should be also noted that the allowed dimensions could also be enlarged further by choosing an electrode material with a higher Lennard-Jones parameter than Cobalt. For instance, Carbon-based material such as graphene or CNT-ribbon sheet would elevate the potential barrier height by nearly one order, thereby making cell dimensions even more flexible.

Electromagnetics Simulation and Discussion

The switching voltages were determined computationally through exhaustive electromagnetic simulations ran on OPERA-3d, a commercial electromagnetic analysis tool developed by Vector Fields. A geometrical model of the proposed memory cell was fed into a Delaunay-based volume mesh generator to create 79,400 linear tetrahedral elements. The finite element method was used on the generated mesh with the switching voltages as boundary conditions to obtain the electric fields, which were then integrated over the entire volume to calculate the electrostatic energy of a given system. The simulation was run on a finite number of coil-electrode separation states within a given switching voltage to yield an electrostatic energy curve. Finally, this process was iterated on a range of different voltages to find the minimum voltage that enables the switching of the memory cell. It was found that carbon nanocoil-memory core cell only needs switching voltages as low as 1 V (Fig 7(a)) to write and 1.5 V to erase (Fig 7(b)). Here the metallic CNC and point contact between CNC and electrode

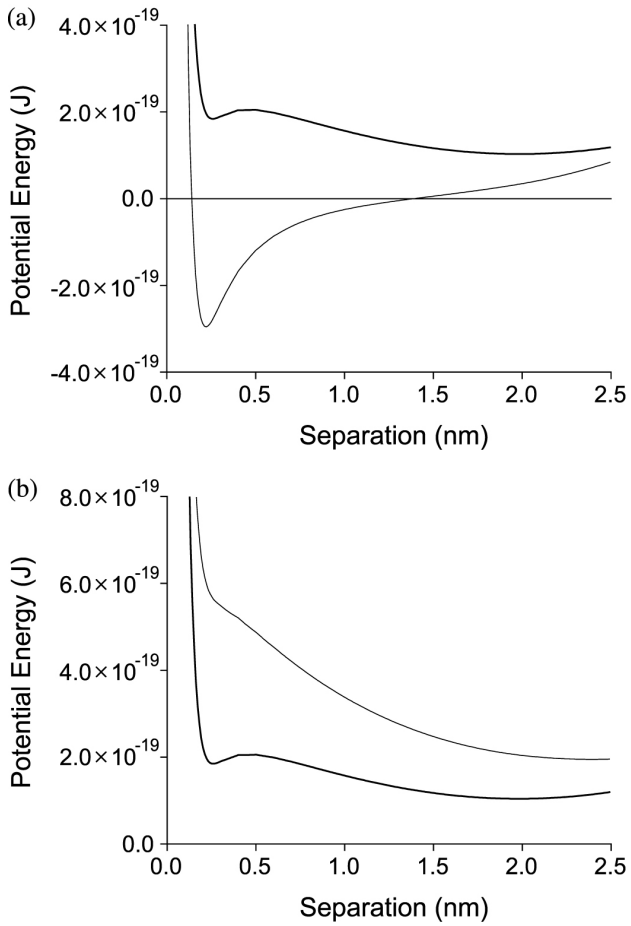

Fig 7. Electrostatic energy curve from Opera electromagnetics simulation added to the original potential energy of the system (a) for data write mode with +1 V and -1 V. Only one potential minimum is present. (b) Same as Figure 5a but for data erase mode with +1.5 V and +1.5 V. The potential barrier is no longer present, which allows the nanocoil to return to its natural state.

was assumed for simplicity of calculation. If the contact area is considered to have a finite size, either the switching voltage of erase mode or the voltage difference between two modes is expected to increase due to a larger van der Waals energy.

During the electromagnetic simulation, it was also found that the floating uppermost electrode plays a critical role in enabling the erase operation of the memory cell. When the same simulation was run with the uppermost electrode removed, even the highest voltage within the failure limits of a carbon nanocoil yielded an electrostatic force that is many orders short of the necessary force to achieve the erase mode. This can be explained by the fact that charges refuse to localize around the nanocoil-electrode contact due to the increasing

repulsive electrostatic force as charges accumulate. On the other hand, the addition of another top electrode dramatically improves the localization of charges due to induced charges of opposite polarity on the uppermost plate, which fortunately does not apply a significant attractive force to the coil during the erase mode due to the Coulomb energy's asymptotic dependence on charge separation.

Nanocoil memory being an electric field-driven device, the extent of crosstalk between neighboring cells in array structure was also investigated. The most serious concern is the effect of electric field along the vertical axis from one device to all other devices along the electrode chosen for switching. Yet, it should be noted that the electric energy depends not only on the distance but also on the effective angle, resulting in an inverse quadratic dependence. The infinite series of the applied electrostatic energy from neighboring cells therefore converges rapidly, as shown in Fig 8(a) for a device with 20 nm cell-to-cell separation and 4 nm coil-to-electrode initial separation. The ratio of these two values entire determines the converged value, which diminishes rapidly with increasing ratio. Fig 8(b) indicates that a 10:1 ratio cuts down the crosstalk effect to a negligible 4%. Considering that a crosstalk effect lower than 50% can be certainly tolerated in the actual device, it was concluded that electrostatic crosstalk should not be a hindering factor in device operation.

The effect of the carbon nanocoil's natural inductance on the device due to its coiled morphology was also investigated. From classical electromagnetics, we can derive the following formula for the inductance of a coil:

$$L_{coil} = N^2 R \mu_0 \mu_r \left[\ln\left(\frac{8R}{a}\right) - 2.0 \right]$$

For a nanocoil with N=10, R/a=5 and R=10 nm, the expected inductance value is 2.1 pH. Assuming a 1 kΩ resistance, we get a time constant of 2.1×10^{-16} sec, which is the time that the system takes to achieve 63.2% of the maximum theoretical current. Immediately we see that the effect of CNC's inductance is negligible for data read operation. By the same token, induced current between nanocoils is negligible, especially with the magnetic field's inverse quadratic dependence.

In contrast to the reading speed, the write and erase speed

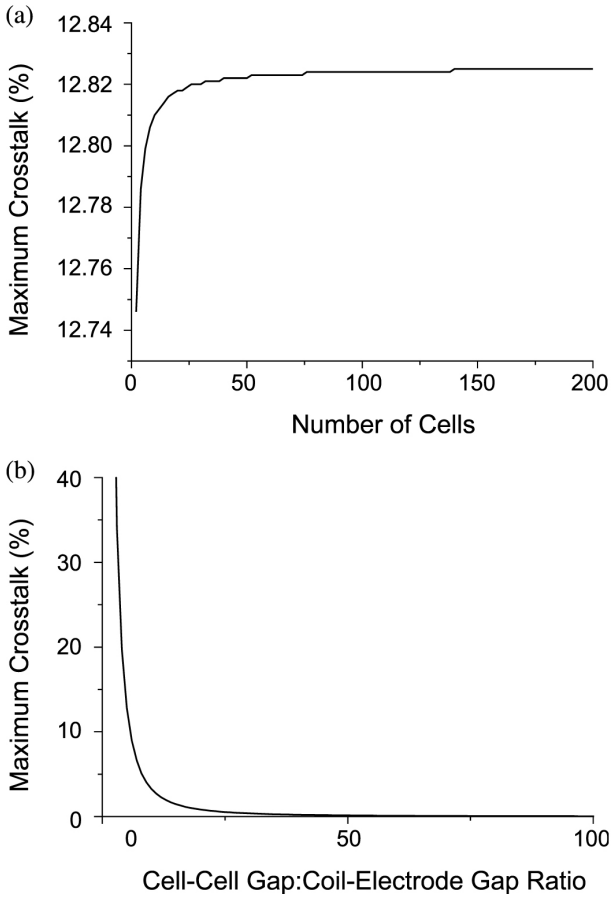

Fig 8. Estimation of cell to cell crosstalk (a) Electric energy crosstalk value rapidly converges with the increasing number of neighboring devices along the electrode. This figure applies to a device with a 5:1 cell separation:coil-electrode separation ratio. (b) Higher cell separation: coil-electrode separation ratio results in lower maximum electric crosstalk value. This figure shows an asymptotic dependence of the convergence value on the separation ratio.

strongly depends on the amount of damping that affects the nanocoil during switching. A critically damped system with a coil 5 nm in diameter and 12 nm in length, however, is expected to have switching times on the order of 10^{-11} sec, ignoring electrode charge time. Underdamped or overdamped systems will have greater operation times but should still be fast enough even for logic applications. Furthermore, besides the damping from the non-ideality of the carbon nanocoil, the amount of viscous damping could be controlled by adjusting the pressure conditions during device fabrication to approach optimal operation.

The memory structure proposed and analyzed above can

be fabricated by modified applications of the photolithography process. The only obstacle to overcome however lies in carbon nanocoil synthesis, which, as with conventional carbon nanotube synthesis, is certainly improving and yet needs further development. Various groups are making efforts to elucidate the physical mechanism of carbon nanotube synthesis (22-24).

Conclusion

The biggest expected merit to build the Random Access Memory (RAM) with the CNCs as the memory core cell is its extremely efficient power consumption. Simulation results indicate that set and reset voltages are both below 2 V. This efficiency can be attributed to the low potential barrier that is used to modulate switching, which is on the order of 10^{-19} J. The energy level is an order smaller than other carbon nanotube-based electromechanical devices (2) and yet much greater than $10k_B$ and therefore unaffected by thermal vibrations. The minimal potential barrier height is achieved by the ideal interplay of carbon nanocoil's extremely low spring constant and a small contact surface between the nanocoil tip and the metal electrode.

Moreover, a nanocoil RAM is expected to be robust as very little stress is exercised on the nanocoils during set or reset operation due to their natural spring-like property. In contrast, significant stress is placed on carbon nanotubes when they are utilized as beams in other nanotube-based electromechanical systems.

As nanocoils are being found at the scale as low as 5 nm in diameter (10), the density of a nanocoil RAM device is only limited by the electrode photolithography technology, which is currently at 40 nm. As a true transistor-less crosspoint array is expected to be possible with this structure, nanocoil RAM's theoretical density lies at a staggering terabit/cm^2 scale. With further development in nanocoil synthesis techniques, the structure hereby proposed promises to be a strong contender for next-generation nanoelectronics.

Acknowledgement

This work was supported by the Tera-level Nano Devices (TND), a research program of the Ministry of Science and Technology, Korea.

References

(1) Iijima S (1991) **354**, 56
(2) Rueckes T (2000) **289**, 94
(3) Baughman RH (1999) **284**, 1340
(4) Dequesnes M, Rotkin SV, Aluru NR (2002) **13**, 120
(5) Han J (1997) **8**, 95
(6) Kim P, Lieber CM (1999) **286**, 2148
(7) Ihara S, Itoh S (1995) **33**, 931
(8) Zhang M, Nakayama Y, Pan L (2000) **39**, 1242
(9) Kuzuya C (2002) , 57
(10) Biro LP (2002) **19**, 3
(11) Zhong DH, Liu S, Wang EG (2003) **83**, 4423
(12) Pan L (2001) 19
(13) Choi WB (2004) **15**, S512
(14) Bajpai V, Dai L, Ohashi T (2004) **126**, 5070
(15) Chen Y (2003) **14**, 462
(16) Choi YH, Kim YK (2004) **15**, S639
(17) Chen X (2003) **3**, 1299
(18) Hayashida T, Pan L, Nakayama Y (2002) **323**, 352
(19) Bachtold A (1998) **73**, 274
(20) Lennard-Jones JE (1930) **129**, 598
(21) Hertel T, Walkup RE, Avouris P (1998) **58**, 870
(22) Motojima S, Chen Q (1999) **85**, 3919
(23) Fonseca A (1996) **77**, 235
(24) Pan L, Zhang M, Nakayama Y (2002) **91**, 10058

(Received March 2, 2006; Accepted March 22, 2006)